



PERSON IDENTIFICATION BASED ON DIFFERENT COLOUR MODELS IRIS BIOMETRIC AND CONTOURLET TRANSFORM

Dhuha Hussein Hameed¹, Prof. Maher Khudhiar Mahmood²

- 1) M.Sc. Student, Electrical Engineering Department, Mustansiriyah University, Baghdad, Iraq.
- 2) Prof., Electrical Engineering Department, Mustansiriyah University, Baghdad, Iraq.

Received 12/ 6/2018

Accepted in revised form 10/ 1 / 2019

Published 1/1/2020

Abstract: Iris identification plays an important role in many applications like security, banking, access to buildings, and surveillance etc. Since the iris part of the eye image can be significantly affected by some factors, such as lighting conditions source, eyelids, eyelashes, pupil, sclera, and shadowing, therefore iris identification research is still wide and rich. The work proposed in this paper operates the iris identification system on the distorted colored images captured under visible light. The proposed idea minimizes the number of iris regions affected by distortion, by dividing the iris region into separable regions. Only the region without distortion part or region with distortion is less probable is used. The paper studies the effect of different color model such as HSV, YIQ, YCbCr, and RGB color models on iris identification. High quality feature extraction is introduced in this paper by using Contourlet Transform (CT). Euclidian Distance (ED) or Neural Network (NN) is used as classifiers. Simulation results show that the proposed method operating on non-distortion iris region outperforms the conventional method operating on the whole iris region for any selected color model and for standard databases (UPOL and UTIRIS) and a suggested one.

Keywords: Colored Iris Identification System, Color Models, Contourlet Transform, Iris Classifier, Neural Network classifier, Euclidean distance classifier.

تحديد هوية الشخص استنادا الى نماذج الالوان المختلفه للقرححية البيومترية والتحويلات الكونتورية

الخلاصة: تحديد الهوية باستخدام قرححية العين يلعب دورا مهما في العديد من التطبيقات مثل الأمن ، والخدمات المصرفية ، والوصول إلى المباني ، والمراقبة ... وبما ان القرححية هي جزء من صورة العين يمكن أن تتأثر بشكل كبير في بعض العوامل، مثل مصدر الإضاءة وانعكاس البيئة المحيطة داخل القرححية اثناء عملية التصوير، وكذلك الجفون، الرموش التي تحجب جزء من القرححية وخصوصا عندما يكون الأشخاص غير متعاونين اثناء عملية التصوير، وأبضا البؤبؤ، والقرنيه التي تكون جزء من القرححية عندما يكون نظام تجزئة التلقائي غير صحيح 100% وبالتالي فان التعرف على الأشخاص باستخدام القرححية لا يزال البحث فيه مستمرا. العمل المقترح في هذه البحث يعمل بنظام تحديد الهوية باستخدام صور القرححية الملونة المشوهة الملتقطه تحت الضوء المرئي. تقلل الفكرة المقترحة من عدد مناطق القرححية المتأثرة بالثشوه ، من خلال تقسيم منطقة القرححية إلى عدد من المناطق. ثم تؤخذ فقط المنطقة التي لا تحتوي على الأجزاء المشوهة أو المنطقة الأقل تشويها. ويتم دراسته تأثير نماذج الالوان المختلفه مثل HSV و YIQ و YCbCr و RGB على تحديد هوية القرححية. وتستخدم التحويلات الكونتورية لاستخراج ملامح القرححية لكل قناة مختارة من مساحة لون مختارة لتقديم ميزة استخراج عالية الجودة. يتم استخدام المسافة التقليديه أو الشبكة العصبية كمصنف. أظهرت نتائج المحاكاة أن الطريقة المقترحة التي تعمل على منطقة القرححية غير المشوهه تفوق الطريقة التقليديه التي تعمل على منطقة القرححية بأكملها، لأي نموذج لون، ولقواعد البيانات القياسية (UPOL) و قاعده البيانات المقترحة (UTIRIS).

1. Introduction

Biometric technologies are automated methods of identifying the person's feature based on a physiological or behavioral characteristic that the person possesses [1]. Recently the term Biometrics has also been used to refer to the emerging field of technology. It is a common and reliable way to identify or verify individuals on the basis of their either physiological characteristics (iris-patterns, fingerprints, face recognition) or behavior characteristics (signature, keystroke, voice) [2]. People can forget password, lose their identity cards that is to be used for identification but they cannot lose or forget their physical characteristics [3]. Iris identification based on physiological characteristics of the iris by extracting the feature pattern of the person's iris, will be discussed in this paper. A good biometric system can be described as Global (each individual must have a special description). Highly unique (the opportunity of any two individuals with similar properties will be small), and Stationary (the person's trait does not alter over time). The identification of the human iris has the characteristic of good biometric system, because of the same individual has non identical irises even between the left and right eye, and also twins have not the same irises due to the epigenetic nature of iris patterns, therefore the iris identification is global and highly unique. Also unique epigenetic pattern of the iris remains stable throughout adult life of the person, therefore the iris biometric is stationary.

Due to these, the iris identification system can be considered as one of the most promising high secure, reliable and stable system compared with other biometric identification systems such as (fingerprints, facial features, voice, hand geometry, and handwriting) systems [4]. Iris identification system consists of image acquisition, iris segmentation, iris normalization, feature extraction, and classifier. The eye image is captured by using color (RGB) camera, the captured image of the eye contains data, derived from the surrounding eye region along with iris as shown in Figure 1.

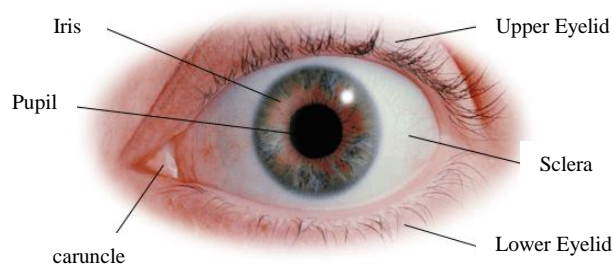


Figure1. eye image acquisition

Therefore, firstly the iris is localized in the segmentation process from the captured eye image. In this paper, an automatic segmentation process based on the circular Hough transform (CHT) is used to find the inner iris circle [5] and Daugman's Integro-differential operator (IDO) [6] is used to find the outer iris circle, at the end of this process, six parameters (center coordinates and radius) for both inner and outer iris circles are determined.

Due to variations in the size of the iris because of pupil dilation from varying levels of illumination (light source), varying imaging distance (camera to the face distance), head tilt, and motivation of the iris within the eye, the iris is normalized to process all these problems. In this paper Daugman's rubber sheet model is employed to normalize the extracted iris area for setting up a constant dimension of the iris area [7]. At the end of this process RGB normalized iris image will be produced. Then each channel of selected color model of the normalized iris image is applied to band pass decomposition for extracted iris information. Do and Vetterli suggested the CT as a new 2-D extension of the wavelet transform (WT) using multi scale and multi directional. This information represents features of iris with more directional information and smooth contour which can be done effectively by computing the CT instead of the WT, due to its properties of directionality and anisotropy [8]. These features are utilized as an input to the classifier. Then identification rate is computed from the classifier output. Figure 2 shows iris identification system block diagram.

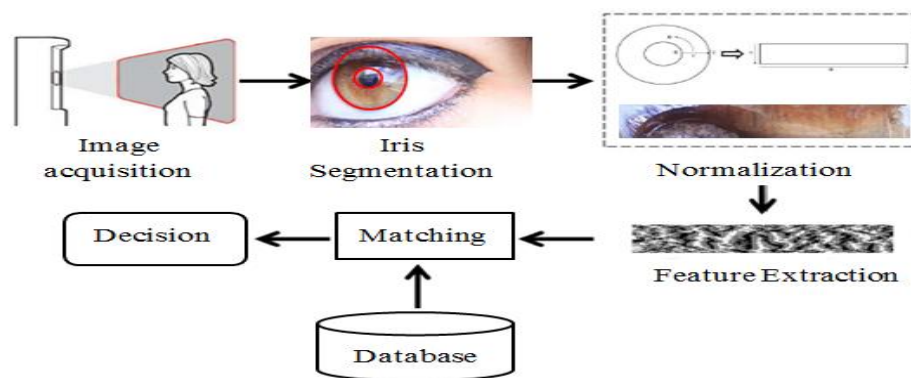


Figure2. Iris identification system block diagram

- There are different types of distortion that corrupt the iris region. These are
- 1-Eyelids: The upper and lower portions of the iris are impeded because of the natural function and movement of the eyelids.
 - 2-Eyelashes: Eyelashes can impede portions of the iris in two different forms as they are shown as grouped or isolated. A uniform darker region is generated in the iris area if the presence of multiple (grouped) eyelashes in the iris areas, or generated as a very thin and darker line in the iris area if one eyelash is isolated.
 - 3-Pupil and sclera: When the inner and outer circles of the iris are not correctly segmented, some portions of the pupil and some portions of the sclera will be considered as iris regions. The pupil zones will be visible at the upper portion of the iris in normalized form, while the sclera zones will be visible at the lower portion of the iris in normalized form.
 - 4-Source light reflections: The regions with “strong reflections” are related to the spectral reflection due to illumination provenance intensity of light sources straight pointed to the iris. These regions have higher intensity values.
 - 5-Shadowing: This type of distortion corresponds to the information that is reflected from the location where the person is placed and is looking at. The regions of this

reflection have lower intensity values related to an extensive range of things that the person is enclosed by [9].

This paper proposes a new method to minimize the number of iris regions affected by distortion, by dividing the iris region into separable regions, and then regions without distortion part are chosen as normalized iris. The paper also studies the effect of different color models on iris identification performance.

The rest of the paper is organized as follows: Section 2 gives an overview of the Color Models. Section 3 explains the proposed method. Section 4 gives an overview of the Contourlet Transform. Iris classifiers are described in section 5. Calculation of the identification rate is explained in section 6. Databases used in this paper are given in section 7. Section 8 shows the simulation results and section 9 presented the conclusions.

2. Color Models

The purpose of the color model is to simplify the specification of colors in some standard. A color model is a specification of a coordinate system and sub-model within the system where each single point in the coordinate system represents a diverse color within the system. Therefore, Color model is a mathematical model that briefly converts the light color into three color components in the three dimensional model using some mathematical functions to explain how the colors are exemplified and specifies the components of color model accurately to learn how each color spectrum looks like. Therefore, the color model can be defined as the digital exemplification of possibly contained colors. A different definition is established to define it as the way to recognize color. Different color models are presented for different applications such as; computer graphics, image processing, TV broadcasting, digital video and computer vision [10].

2.1. RGB color model

The RGB color model is the most appropriate and popular model for processing digital images. The RGB color model has been derived from three primary additive colors, which are (Red, Green, and Blue). These colors are combined in predefined proportions to produce the full range of colors. Therefore, this model is called additive color model [10]. The cube of RGB color model is shown in Figure 3.

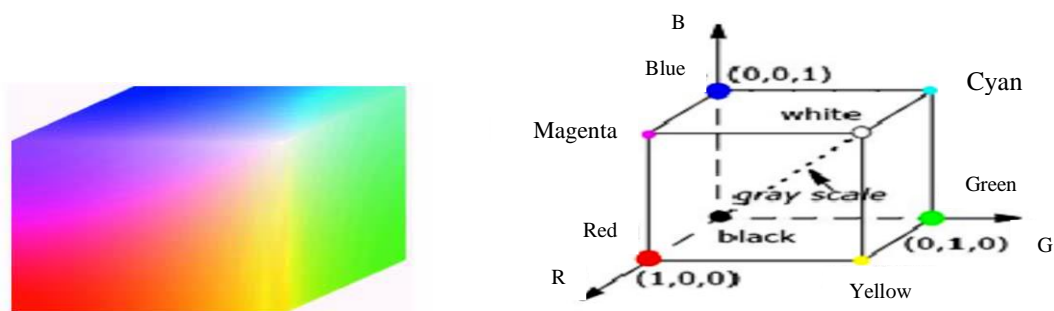


Figure3. RGB color model[10]

Despite the RGB model is widespread, it has a major drawback: a small change in illumination change RGB coordinates significantly, because its intensity images combine both the color and illumination information. For example, taking a photo of a green surface with and without a source of light (change illumination conditions) the results are two images, where pixel values differ significantly between these two images even though color stayed the same. Usually the illumination conditions change between different samples of the same iris. It might affect significantly identification rate. Therefore, another color model which separates the illumination information from the color information must be introduced.

2.2. HSV color model

The Hue Saturation Value (HSV) color model is also known as Hue, Saturation Brightness (HSB). Hue channel (H) refers to the pure color with ranges from 0 - 360, where each value corresponds to one color. Saturation channel (S) is the intensity of the color, refers to the relative purity or the amount of white light mixed with a hue. Value channel (V) is the measurement of brightness of color, ranging from 0 – 1. Figure 4 shows the HSV color model [10]. The transformation that converts the RGB color model to HSV color model is given by:

$$H = \begin{cases} \theta & \text{if } B \leq G \\ 360 - \theta & \text{if } B > G \end{cases} \quad (1)$$

$$\theta = \cos^{-1} \left\{ \frac{\frac{1}{2}[(R-G)+(R-B)]}{[(R-G)^2+(R-B)(G-B)]^{1/2}} \right\} \quad (2)$$

$$S = 1 - \frac{3}{(R+B+G)} [\min(R, G, B)] \quad (3)$$

$$V = \frac{1}{3}(R + G + B) \quad (4)$$

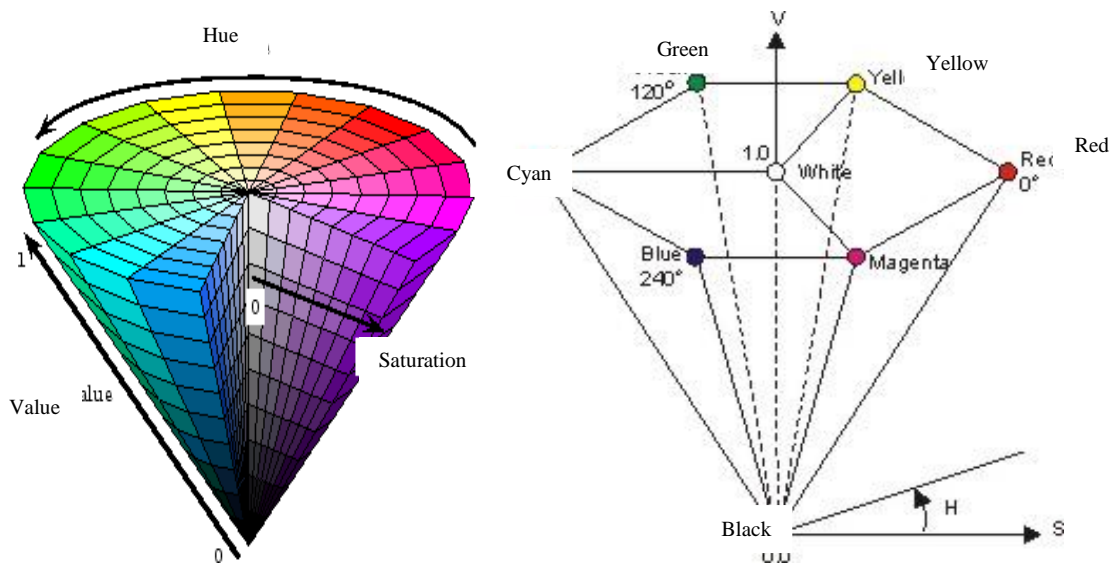


Figure4. HSV color model[10]

2.3. YCbCr Color Model

The Y component is the luminance channel representing light intensity which is the gray scale information, Cb (Chroma blue) and Cr (Chroma red) are representing the Chrominance channels, which are color information. Figure 5 shows YCbCr color model [10]. The transformation that converts the RGB color model to YCbCr color model is given by:

$$\begin{bmatrix} Y \\ C_b \\ C_r \end{bmatrix} = \begin{bmatrix} 16 \\ 128 \\ 128 \end{bmatrix} + \begin{bmatrix} 65.481 & 128.553 & 24.966 \\ -37.797 & -74.203 & 112 \\ 112 & -93.786 & -18.214 \end{bmatrix} \begin{bmatrix} R \\ G \\ B \end{bmatrix} \quad (5)$$

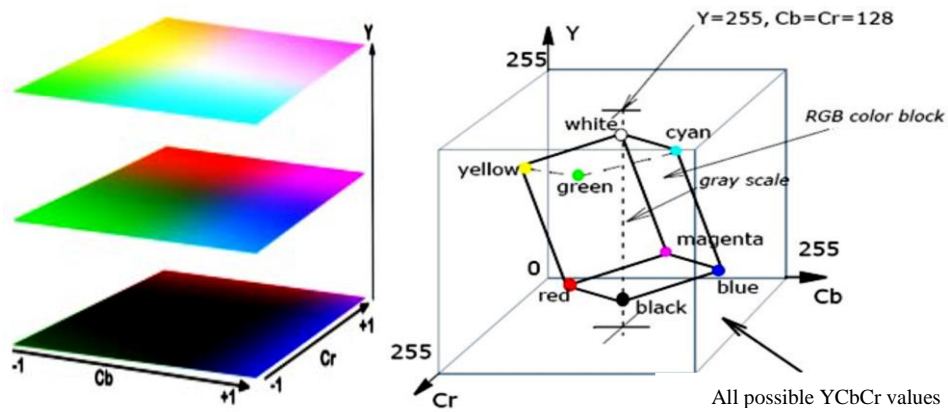


Figure5. YCbCr color model [10]

2.4. YIQ Color Model

The Y is the luminance channel representing light intensity, I (in-phase) and Q (quadrature) chrominance channels representing color details. The Y component can be represented as a combination of Red, Green and Blue intensities. The I channel encompasses the band of Orange-Cyan hue information and the Q channel encompasses the band of Green-Magenta hue information [10]. Figure 6 shows YIQ color model. The transformation that converts the RGB color model to YIQ color model is given by:

$$\begin{bmatrix} Y \\ I \\ Q \end{bmatrix} = \begin{bmatrix} 0.299 & 0.587 & 0.114 \\ 0.596 & -0.274 & -0.322 \\ 0.212 & -0.523 & 0.311 \end{bmatrix} \begin{bmatrix} R \\ G \\ B \end{bmatrix} \quad (6)$$

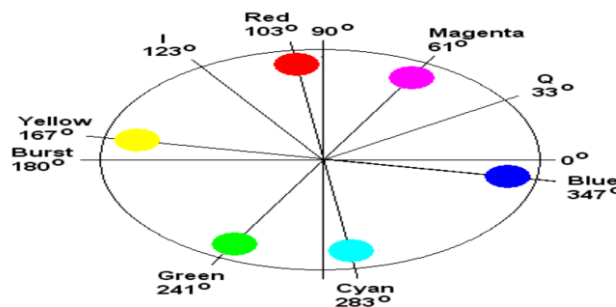


Figure6. YIQ color model [10]

3. Proposed Method

In the robust image capturing requirements, it is feasible to get good quality images and achieve high identification rates. However, these identification rates largely decrease, when the images do not have enough quality, or due to focus, contrast, or brightness problems and iris obstructions or reflections. Getting high quality iris image requires the person to stand close (less than two meters) to the imaging camera and wait for a period about three seconds until the data is captured. This cooperative behavior is required in order to capture images with enough quality for the identification task. This cooperative behavior is considered as a weak point, it powerfully restricts the range of domains where iris identification can be used, especially when the person is not cooperated.

Images captured at a distance, without effective involvement of the person and at low controlled lighting situation lead to increase the probability of taking extremely diverse images related to focus, brightness and contrast with several other types of information in the captured iris regions such as iris obstruction by eyelids or eyelashes, reflections and shadowing. All these factors are considered as distortion. Therefore the proposal of this paper is to increase the iris identification robustness to these distortions located in the iris region.

In this paper the iris region is divided by taking only the portions that are not corrupted by distortion such as spectral reflection, lighting, shadowing, glasses, iris obstruction by eyelids and eyelashes (due to no cooperative imaging environments) and pupil and sclera (due to less accurate iris segmentation), which lead to iris regions corrupted by distortion. Under natural lighting conditions, we observed that the most common types of distortion (iris obstructions, reflections and shadowing), reflection and shadowing are predominant, respectively, in the inner and outer iris regions, while iris obstructions are predominantly in the upper and lower parts of the iris regions.

Due to these distortions, the iris is divided into separable regions and makes the decision of identification based upon small regions that do not contain any distortion factors. This means that only points from selected portion is used to generate the strip representation. This portion is confined between two angles θ_1 and θ_2 . These two angles must be the same for each person and may be different between persons in the database.

This depends on the distortion location in the iris image. To allow a comparison between all persons in the database, all persons must have iris normalized image with the same different angles ($\theta_2 - \theta_1$). The proposed division strategy minimizes the iris region affected by distortion, giving higher identification rate. Figure 7 shows the portions of the iris region depending on the angles (θ_1 and θ_2).

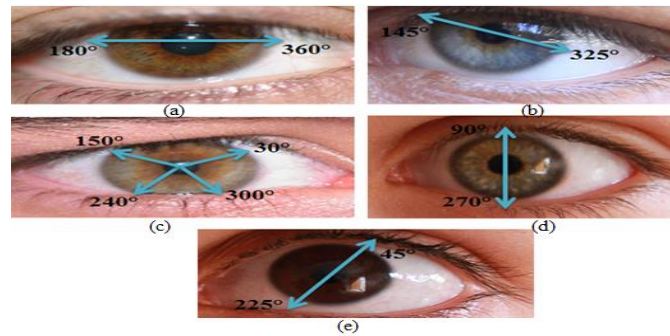


Figure7. (a) Normalized iris from $[180^\circ, 360^\circ]$. (b) Normalized iris from $[145^\circ, 325^\circ]$. (c) Normalized iris from $[300^\circ, 30^\circ]$ and $[150^\circ, 240^\circ]$. (d) Normalized iris from $[90^\circ, 270^\circ]$. (e) Normalized iris from $[45^\circ, 225^\circ]$.

In the Figure 7a, the upper portion from ($\theta_1 = 0^\circ$ to $\theta_2 = 180^\circ$) or the lower part from ($\theta_1 = 180^\circ$ to $\theta_2 = 360^\circ$) are chosen. The size of each part is half the reference size of the whole normalized iris, but this case is not a particular case because the upper and lower parts of the iris region are usually occluded by eyelids and eyelashes. Therefore, this case will be chosen for eye images not under the effect of the eyelids and eyelashes or at least will be chosen for eye images where the lower part of the iris is not occluded by eyelids or eyelashes.

In Figure (7b), the portions of the iris region from ($\theta_1 = 145^\circ$ to $\theta_2 = 325^\circ$), or from ($\theta_2 = 325^\circ$ to $\theta_1 = 145^\circ$) are chosen. The size of each portion is half the reference size of the whole normalized iris. Choice of the iris part depends on the distortion location. In Figure (7c), the iris region is divided into the four portions $[30^\circ, 300^\circ]$, $[30^\circ, 150^\circ]$, $[150^\circ, 240^\circ]$ and $[240^\circ, 300^\circ]$. The $[300^\circ, 30^\circ]$ and $[150^\circ, 240^\circ]$ portions are taken together, to make the size of normalized iris half the size of whole normalized iris, to have a comparison with other two cases in Figure (7a) and Figure (7b). Therefore, the normalized iris images must be the same size for all persons in the database. In this case, the normalized iris in $[30^\circ, 150^\circ]$ and in $[240^\circ, 300^\circ]$ are most affected by eyelids and eyelashes distortion. Hence, these portions will be ignored, taking normalized iris from $[300^\circ, 30^\circ]$ and $[150^\circ, 240^\circ]$ together. In Figure (7d), the portions of the iris region from ($\theta_1 = 90^\circ$ to $\theta_2 = 270^\circ$), or from ($\theta_2 = 270^\circ$ to $\theta_1 = 90^\circ$) are chosen.

The size of each portion is half the reference size of the whole normalized iris. Choice of the iris part depends on the distortion location. In Figure (7e), the portions of the iris region from ($\theta_1 = 45^\circ$ to $\theta_2 = 225^\circ$), or from ($\theta_2 = 225^\circ$ to $\theta_1 = 45^\circ$) are chosen. The size of each portion is half the reference size of the whole normalized iris. Choice of the iris part depends on the distortion location. Therefore the whole iris between $[0^\circ, 360^\circ]$ is not transformed in the proposed system, instead only selected unaffected portions are used. Figure 8 shows the normalization step for different angles of RGB color model image.

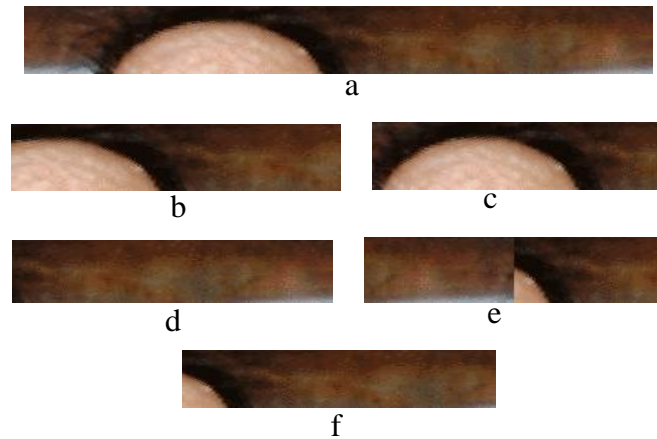


Figure8. Normalization iris image for different angle division (a): $[0^\circ, 360^\circ]$. (b): $[90^\circ, 270^\circ]$. (c): $[45^\circ, 225^\circ]$. (d): $[180^\circ, 360^\circ]$ (e): $[300^\circ, 30^\circ]$ & $[150^\circ, 240^\circ]$. (f): $[145^\circ, 325^\circ]$.

From Figure 8, it is clear that the best selection of the normalized iris image is the angle from $[180^\circ, 360^\circ]$.

4. Iris Feature Extraction

The feature representation should have enough information to be able to classify the different irises and must be less sensitive to noise. In this paper, a new technique which is the extension of the wavelet transform is used, it is named as Contourlet Transform CT. The iris normalization image (strip shape) is decomposed by CT. The low and high frequency sub bands are obtained. The feature vector can be either low frequency sub band or any high frequency sub band for direction level at each decomposition level.

4.1 Contourlet Transform (CT)

CT is developed by Do and Vetterli, it is a new exemplification for 2D images, expansion of WT, using multi-scale and directional filter banks that can capture the effective geometrical structure (smooth contour and fine details) of information. The CT consists of two parts. They are Laplacian Pyramid (LP), and Directional Filter Bank (DFB). The combination of these two parts is known as Contourlet Transformation or Pyramidal Directional Filter Bank (PDFB). Contourlets were advanced for obtaining effective information from the contour pattern segments of an image and overcoming the restrictions of conventional wavelets in this respect, with flexible aspect ratio that produces a rich set of the basis images [11]. Figure9 shows the construction of the CT. First the image is applied to multi-scale decomposition to produce the coarse image which contains the low frequency information, and band-pass image which contains the abrupt points of the image then this band-pass image is applied to linear structure DFB.

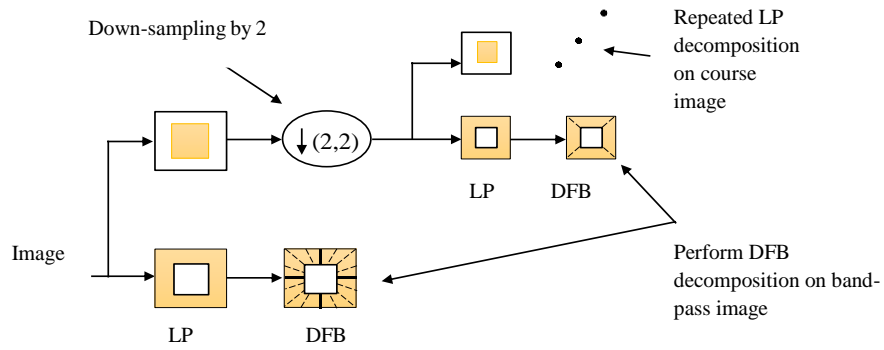


Figure9. Construction of Contourlet Transformation

4.1.1 Multi-scale Decomposition

Laplacian pyramid (LP) is one of the ways used to achieve a multi scale analysis, presented by Burt and Adelson. Decomposing image by LP can be done by down sampling the low pass version (analysis filter) of the original image that gives the coarse image. Then low pass version (synthesis filter) of the up sample of the coarse image gives the predicted image. Then the difference between the original image and the predicted image results in the band pass image. Figure10 clarifies the one level decomposition of LP procedure, where both (H) and (G) are low-pass filters in analysis and synthesis stages respectively, and M is the sampling matrix. The procedure can be re-iterated on the coarse image [11].

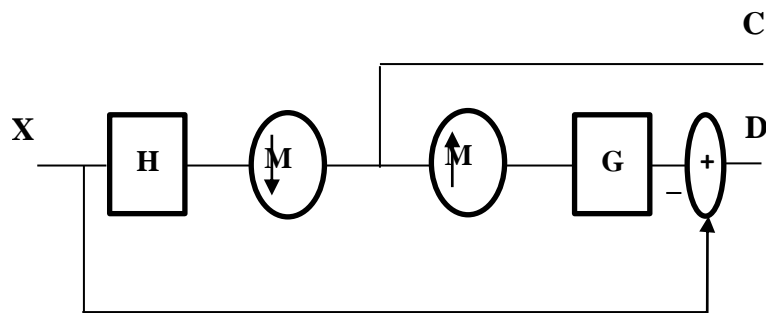


Figure10. LP one level Decomposition process

4.1.2 Directional Decomposition

Directional filter bank was proposed by Bamberger and Smith. The directional filter bank provides maximum decimated sub band and sensitive direction of 2D image. The perfect reconstructed (synthesis) of the image can be achieved. Directional filter bank is implemented by l -level binary tree decomposition. These decompositions lead to 2^l directional sub bands [12]. The wedge edge shaped frequency partitioning of directional component of the image is shown in Figure11.

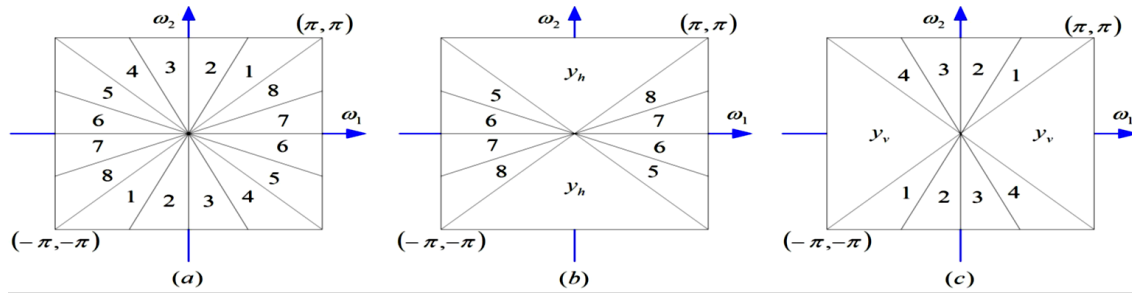


Figure11. Partitioning of frequency spectrum (a) Partitioning of frequency spectrum using three-level (full-tree) DFB; Examples of frequency partitioning using three-level (b) vertical and (c) horizontal filter bank, VDFB and HDFB, respectively [13]

CT decomposition images are obtained, where $L = [l_1, l_2, l_3, l_4 \dots \dots l_j]$, l_j is decomposition level of DFB in the j^{th} level of LP.

For $L=[2,3,4]$, the CT decomposition result are low frequency sub band, four high frequency directional sub bands, eight high frequency directional sub-bands, and sixteen high frequency directional sub bands as shown in Figure12.

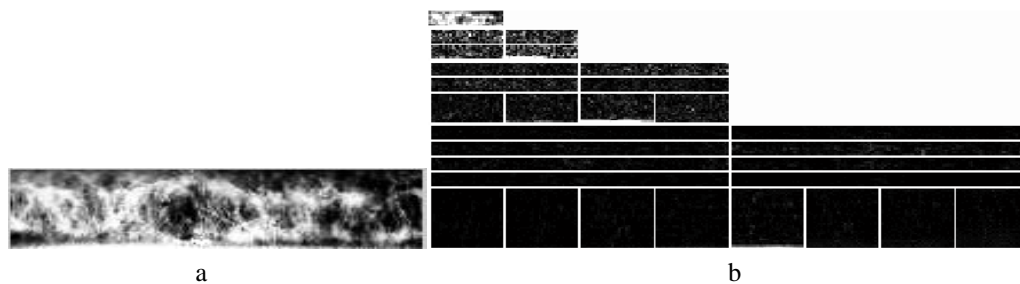


Figure12. CT decomposition. (a) Green channel iris normalized image. (b) Sub bands of CT.

The CT decomposition will be applied on each channel of selected color space of normalized iris image, and the low frequency sub-bands is used as a feature vector.

5. Iris Classifier

The classifier needs a feature selection that is extracted by CT to comprise information demand to assort between classes. In this paper, two types of classifiers are tested, these are ED or MLNN.

5.1. Euclidean Distance Classifier

The ED classification performance is based on distance value given by:

$$ED = \sqrt{\sum_{i=1}^N (x_i - y_i)^2} \tag{7}$$

Where: N is the length of feature vector, x_i is feature vector of the test image, and y_i is feature vector of any image in the database [14]. To produce the feature vector for

the color image, each channel of selected color model is decomposed by CT, and then the selected frequency coefficient from the decomposition result is used as feature vector. Then the combined features of each channel produce the feature vector of color image.

To identify one image in the database, the distance matrix is needed. This has size of the number of image per person times number of persons. Then minimum value of the distance matrix will identify the person.

Suppose that $D(I, T_{ij})$ is the distance matrix between the feature vector of test normalized iris image I and feature vector of any other normalized iris image T_{ij} of the i^{th} normalized iris image of the j^{th} person, $i=1,2,\dots, M$, where M is the number of normalized iris image for each person. And $j=1, 2,\dots, N$, where N is the number of persons, and suppose $D(I, T_j)$ is the minimum value in the distance matrix $D(I, T_{ij})$ which is given by Equation (8), that identifies which j^{th} person that the testing image belongs to him.

$$D(I, T_j) = \min_{i=1,2,\dots,M} \{D(I, T_{ij})\} \quad j = 1, 2, \dots, N \quad (8)$$

5.2. Neural Network classifier

A simple multilayer neural network (MLNN) may also be used as a classifier. The number of the neurons in the input layer equals the size of feature vector, while the number of the neurons in the output layer is equal to the classes of the database. The number of the neurons in the hidden layer is experimentally optimized relying on the intricacy of the ID problem. In the neural classifier, the database is divided in two groups, the training set images (seen images) and testing set images (unseen images). To train the neural network two types of data are needed, feature matrix and desired (target) matrix. To produce the feature matrix, each channel of selected color model for each image in the training stage is decomposed by CT at different scales and various directional levels, and then the selected frequency coefficient is used as feature vector. Then for all training images, a feature matrix has size equals $(n \times k \times \text{number of images in the training set})$ where k is the length of the feature vector for one channel, and n is the number of channels. The desired matrix has size of number of persons times number of images in the training stage, and it is compared with actual output matrix; if these matrices are not equal, the weights should be changed to minimize this. At first, the weights values are randomly selected. Then the weights are adapted at each epoch (iteration) to minimize the difference between the actual output matrix and the desired (target) matrix, in order to minimize the mean square error. Therefore, the training process is continued until the error between the actual output and the desired output is below some threshold value (ε) or the maximum number of iterations is reached. When a new input image from testing group is presented to the classifier, the features of each channel of selected color model of this image are extracted by applying the CT, and then the position of the highest value output determines the class.

6. Calculation of the Identification rate

The ID rate of an individual can be calculated as:

$$p_k = \frac{\text{number of correct identified test images}}{\text{total number of test images}} \quad (9)$$

Where, p_k is the ID rate for k^{th} class of database.

The average ID rate for overall system is given by the following equation:

$$\text{Average ID rate} = \frac{p_1 + p_2 + \dots + p_u}{u} \quad (10)$$

u : is the number of persons in the database

7. Database Preparation

7.1. UPOL

The UPOL database is collected from 64 classes with 3 images per person per eye (i.e. 3x64 left and 3x64 right). Therefore, it is composed from 384 digital color iris images with a size of 576x768 pixels [15]. Figure13 shows some example for UPOL iris database for left eyes.

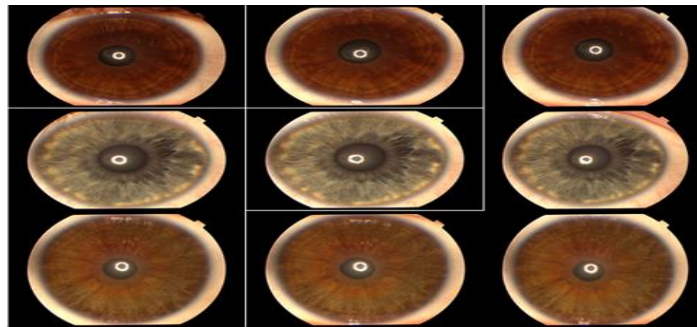


Figure13. UPOL iris images database.

7.2. UTIRIS database

This consists of 1540 images from 79 persons with five images for each person for both left and right eyes in two sessions, which are visible wavelength (VL) imaging (multispectral imaging), and near infrared (NIR) imaging. With number of pixels are 2048x1360 for VL imaging and 1000x776 for NIR imaging. This iris database suffers from upper and lower eyelids and eyelashes distortion also from imaging spectral reflection and multi focus images per person. Therefore the pupil size is changed through images per person. In this paper, the multispectral imaging iris database of right side is used to perform the experiment. Figure14 shows some samples for UTIRIS iris database for VL imaging for right eyes.

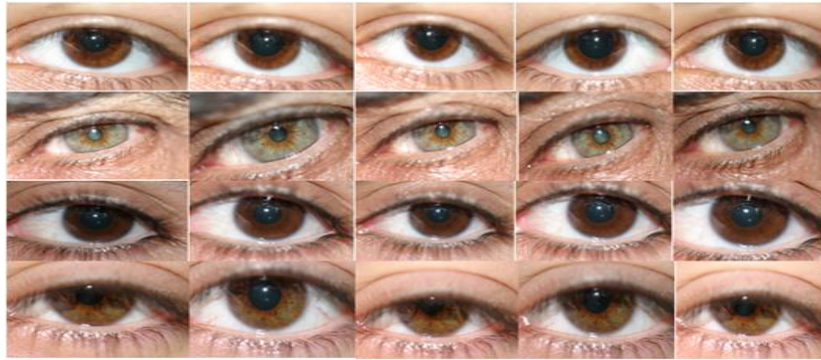


Figure14. UTIRIS iris images database

7.3. Suggested database

A suggested database is prepared to test the robustness of the proposed system against reflection, shadowing and obstruction factors. This database consists of 22 persons each one has 20 different RGB iris images of their left eye with size of 200x400 pixels. The images have been taken for students, at the Electrical Engineering Department, Mustansiriyah University, Baghdad-Iraq. These images are captured at low controlled lighting situation, and without effective involvement of the classes. Therefore, the probability of taking various pictures (concerning focus, brightness or contrast) and with diverse distortion factors (iris impediment, reflections and shadowing) will be increased. Figure 15 shows some images for the Suggested database.

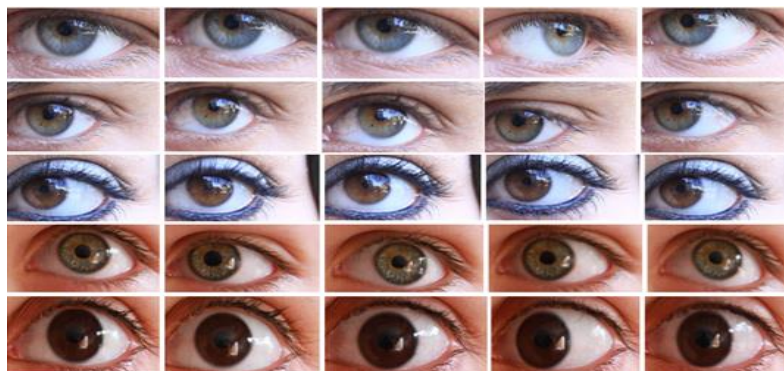


Figure15. Suggested iris images database.

8. Simulation Results

This section is carried out by experiments using RGB, HSV, YIQ and YCbCr color models with CT low frequency sub band for iris identification. The size of normalized iris image is 50x360 and 50x180 for conventional and proposed methods respectively. To perform iris identification on RGB color model, each channel of the RGB color normalized iris images are enhanced with histogram equalization and noise filtering in order to avert the influence of spectral reflection due to illumination provenance intensity on normalized iris. To perform the iris identification on HSV, YIQ and YCbCr color models, the RGB normalized iris image will be converted to select color model then each channel of the color model will be enhanced with noise filtering and only the illumination channel will use histogram equalization for enhancement from light source

level change during imaging. This section determines the best color model for each testing database, where each color model channels are used together, which means that the texture and color of the iris will be considered for each color model.

8.1. Color Iris Identification based on Euclidean Distance Classifier

When performing the identification process, we choose the low frequency sub band for each selected channel of selected color model, after 1 level LP decomposition as features of the normalized iris image.

Tables (1a), (1b), & (1c) show the identification rate of different color models for UPOL, UTIRIS & suggested databases respectively based on ED classifier.

Table (1a) Identification Rate of different color model for UPOL database of testing the Low frequency sub-band of 1st level

Color model	UPOL database	
	Conventional method %	Proposed method%
HSV	100%	100%
YIQ	100%	100%
YCbCr	100%	100%
RGB	100%	100%

The UPOL iris database is perfect database that does not suffer from any distortion type in the iris region, therefore the all color model perform full identification rate of 100%.

Table (1b) Identification Rate of different color models for UTIRIS database of testing the Low frequency sub-band of 1st level

Color model	UTIRIS database	
	Conventional method %	Proposed method%
HSV	83.55%	96.52%
YIQ	77.85%	93.04%
YCbCr	76.89%	93.67%
RGB	80.38%	95.26%

From Table (1b) it is clear that the HSV color model is better in performance than YIQ, YCbCr and RGB color models for both conventional and proposed methods. And the RGB color model is better in performance than YIQ and YCbCr color models for both conventional and proposed methods.

Table (1c) Identification Rate of different color models for Suggested database of testing the Low frequency sub-band of 1st level

Color model	Suggested database	
	Conventional method %	Proposed method%
HSV	99.385%	99.59%
YIQ	98.13%	99.8%
YCbCr	97.5%	99.59%
RGB	97.92%	99.59%

From Table (1c) it is clear that the HSV color model performed best identification rate than YIQ, YCbCr and RGB color models for conventional method, while for proposed method the YIQ color model gives best identification among HSV, YCbCr and RGB color models.

8.2. Color iris identification based on Neural Networks

In the NN classifier each selected channel from any selected color model is resized to 64×256 for conventional method and resized to 64×128 for proposed method in order to be processed by the CT for feature extraction. When performing the identification process, we choose the low frequency sub band as features of the normalized iris image for selected channel of selected color model, after 3 levels LP decomposition with $2^2, 2^3, 2^4$ different directions in level 1, level 2, and level 3 respectively.

This section determines the best color model selection for each testing database. Tables (2a), (2b), and (2c) show the identification rate of different color models for different databases with five independent training runs of NN classifier and the number of (training, testing) images are (2, 1), (3, 1) and (10, 10) for UPOL, UTIRIS and suggested database respectively. The NN is trained by using Mean squared normalized error performance function, with two layers (one hidden layer, and output layer). Number of neurons in hidden layer is 400 neurons and number of neurons in input layer is length of feature vector. The transfer function is TANSIG (tan sigmoid) and Training algorithm is TRAINSCG (Scaled Conjugate Gradient). Figure16 exhibits the block diagram of the NN implemented for simulation.

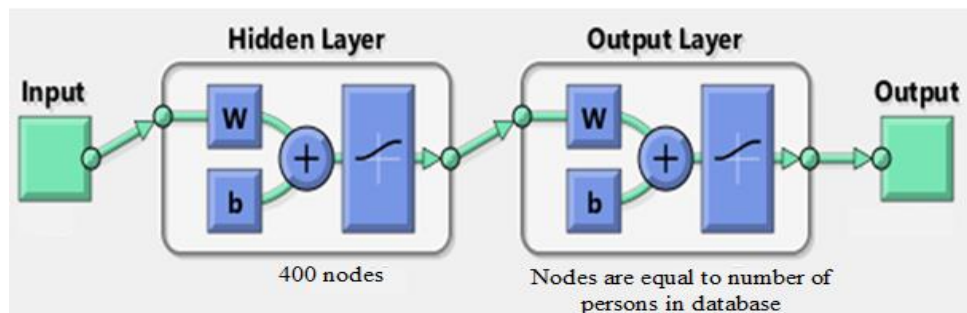


Figure16. Block diagram of MLNN for simulation of iris identification System.

Table (2a) Identification Rate of different color model for UPOL database of testing the Low frequency sub-band of 3th level

Color model	UPOL database	
	Conventional method %	Proposed method%
HSV	98.43%	98.43%
YIQ	100%	100%
YCbCr	100%	100%
RGB	100%	100%

From Table (2a) we see that the identification rate of UPOL iris database on YIQ, YCbCr and RGB color models is greater than HSV color model for both conventional and proposed methods.

Table (2b) Identification Rate of different color models for UTIRIS database of testing the Low frequency sub-band of 3th level

Color model	UTIRIS database	
	Conventional method %	Proposed method%
HSV	94.94%	97.98%
YIQ	90.1%	97.21%
YCbCr	85.06%	92.15%
RGB	85.32%	94.99%

From Table (2b) it is clear that the identification rate of UTIRIS iris database on HSV color model is better than YIQ, YCbCr and RGB color models for both conventional and proposed methods.

Table (2c) Identification Rate of different color models for Suggested database of testing the Low frequency sub-band of 3th level

Color model type	Suggested database	
	Conventional method %	Proposed method%
HSV	98.04%	99.58%
YIQ	96.91%	99.66%
YCbCr	95.84%	99.49%
RGB	95.33%	99.5%

From Table (2c) it is clear that the identification rate of Suggested database on HSV color model is better than YIQ, YCbCr and RGB for conventional method and on YIQ color model is better than HSV, YCbCr and RGB color models for proposed method.

Figure (17) and (18) show the average rates of all tested databases based on CT low frequency sub band with 1 level LP and ED classifier using RGB, HSV, YIQ and YCbCr color spaces for conventional and proposed method respectively.

Figure (19) and (20) show the average rates of all tested databases based on CT low frequency sub band with 3 level LP and NN classifier, using RGB, HSV, YIQ and YCbCr color spaces for conventional and proposed method respectively.

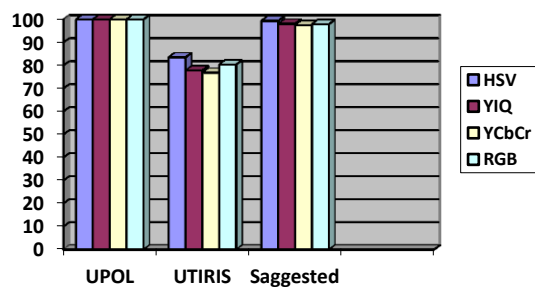


Figure17. Conventional Identification rate of different color spaces for different databases based on ED classifier

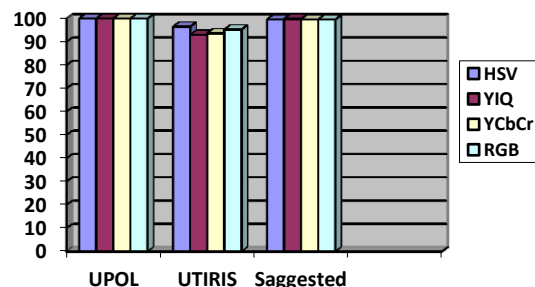


Figure18. Proposed Identification rate of different color spaces for different databases based on ED classifier

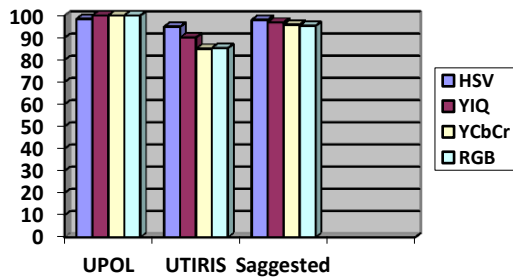


Figure19. Conventional Identification rate of different color spaces for different databases based on NN classifier

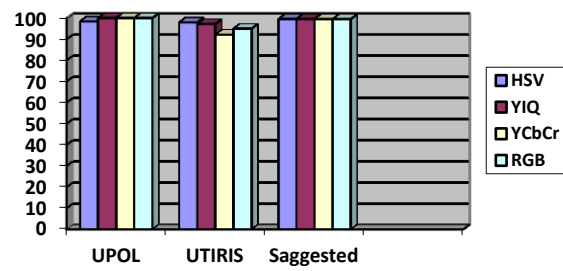


Figure20. Proposed Identification rate of different color spaces for different databases based on NN classifier

9. Conclusions

This paper presented a new algorithm that divides the normalized iris image into separable regions and then makes the identification rate based on region without distortion or region with less distortion results show that the proposed method operating on non-distorted iris region outperforms the conventional method operating on the whole iris region for any selected color model for different database. The optimal color model is different with different database this depended on color and database characteristics. Therefore, the optimal color model of proposed method for UTIRIS database and suggested database are HSV and YIQ for both ED and NN classifier.

10. References

1. J. Wayman, A. Jain, D. Maltoni and D. Maio, (2005), "An Introduction to Biometric Authentication Systems" Biometric systems technology, design and performance evaluation, Springer, XIV, 370P.
2. M. Daris F. and Dr. A. Anthony Irudhayaraj, (2011), "Biometric System" 3rd IEEE International Conference on Electronics Computer Technology, Kanyakumari, India, 8-10 April.
3. S. Anicham, C. Murukesh, (2014), "An Efficient Iris Recognition System Using Contourlet Transform and Neural Networks", vol. 3, issue. 4, April.
4. A. Kumar and A. R. Asati, (2014), "Iris Based Biometric Identification System" IEEE International Conference on Audio, Language and Image Processing, Shanghai, China, 7-9 July.
5. Noraini Abdul Jalil, Rohilah Sahak, and Azilah Saparon, (2012), "Iris Localization Using Colour Segmentation and Circular Hough Transform" IEEE-EMBS Conference on Biomedical Engineering and Sciences, Langkawi, Malaysia, 17-19 Dec.
6. John Daugman, (2004), "How Iris Recognition Works", IEEE Transactions on Circuits and Systems for Video Technology, vol. 14, issue 1, 30 January.
7. Ryszard S. Choras, (2007), "Iris image recognition", 6th IEEE International Conference on Computer Information Systems and Industrial Management Applications (CISIM'07), Minneapolis, MN, USA, 28-30 June.

8. Y. Zhai, J. Gan, J. Zeng, Y. X. (2010), "A Novel Iris Recognition Method Based on the Contourlet Transform and Biomimetic Pattern Recognition Algorithm", IEEE 10th International Conference on signal processing proceedings, Beijing, China, 24-28 Oct.
9. Hugo P. and L.A. Alexandre, (2006), "A Method for the Identification of Noisy Regions in Normalized Iris Images", 18th IEEE International Conference on Pattern Recognition (ICPR'06), Hong Kong, China, 20-24 Aug.
10. Noor A. Ibraheem, Mokhtar M. Hasan, Rafiqul Z. Khan, and Pramod K. Mishra, (2012), "Understanding Color Models: A Review", vol. 2, no. 3, April.
11. C.M.Patil and SudarshanPatilkulkarni, (2010), "An Efficient Process of Recognition of Human Iris based on Contourlet Transforms" ScienceDirect, Procedia Computer Science.
12. DO M.N., Vetterli M., (2005), "The Contourlet transform: an efficient directional multiresolution image representation", IEEE Transactions on Image Processing 14(12), pp. 2091 –2106.
13. Y. Zhang, Q. Z. Li and S. Negahdaripour, (2015), "Seafloor Image Compression Using Hybrid Wavelets and Directional Filter Banks" IEE OCEANS 2015 - Genova, Genoa, Italy, 18-21 May.
14. Abhilasha S. Narote and Laxman M. Waghmare, (2017), "Color Iris Authentication using Color Models" volume 159 – no 2, February.
15. Michal Dobeš and Libor Machala, Iris Database, <http://www.inf.upol.cz/iris>.